PROCEEDINGS, Twenty-Fifth Workshop on Geothermal Reservoir Engineering
Stanford University, Stanford, California, January 24-26, 2000
SGP-TR-165

# UPDATE FLUID FLOW MODEL FOR THE CP1 AREA OF THE CERRO PRIETO GEOTHERMAL FIELD

Marco H. Rodríguez, Héctor Gutiérrez Puente and Jesús de León V.

Comisión Federal de Electricidad, Residencia General de Cerro Prieto
Carretera Pascualitos-Pescaderos Km. 26.5, Cerro Prieto, B.C.
Mexicali, Baja California, Mexico
e-mail: helio@cfe.gob.mx

## ABSTRACT

A fluid flow model for the Cerro Prieto 1 area (CP1) has been updated, on the basis of reservoir engineering and production data collected since 1973. Two reservoirs have been identified in the CP1 area, the shallow alpha and the deeper beta reservoir which extends over the entire field.

Due to 28 years of continuous exploitation and the existence of hydraulic communication between the reservoir zones and the surrounding groundwater aquifers, inflow of cold water into the CP1 reservoirs has occurred. This recharge has been intense in the beta reservoir in the northern part of CP1, and in the alpha reservoir in the southern part. The cold water inflow into the CP1 area has been induced not only by production in CP1, but also by that in the eastern areas of the field (CP2 and CP3).

At present, the most stable productive zone in CP1 is the northern part of the alpha reservoir. The production zone with highest steam quality is in the southern beta reservoir, next to the CP2 area.

## INTRODUCTION

The Cerro Prieto geothermal field, located in the Mexicali Valley of the state of Baja California, about 35 km south of the US-Mexico border, has been producing electrical power since March 1973. The first exploited area is called CP1, in the western part of the field. The area presents two geothermal production zones, the shallow (at 1000 to 1500m depth) alpha and the deeper (below 1500m depth) beta reservoir (Sánchez and de la Peña, 1981). Previous fluid flow models of Cerro Prieto were mainly based on the analysis of lithologic and temperature logs (e.g., Halfman et al., 1982, 1986; Lippmann et al., 1991).

The reservoir response to exploitation has been extensively discussed in several papers (e.g., Mercado, 1976; Truesdell et al., 1979, 1989, 1997; Grant et al., 1984; Truesdell and Lippmann, 1998).

Here more details of the fluid flow model for the CP1 area are presented based on the analysis of (1) reservoir characteristics, (2) fluid production and enthalpy history, (3) chemical and isotopic changes, (4) injected fluid returns, and (5) water level, pressure history and temperature logs. The data and study results will be discussed for different CP1 reservoir zones.

## CP1 RESERVOIR ZONES

The CP1 reservoirs have been subdivided into five zones (i.e., alpha north (αN), beta north (β1N), alpha south (αS), beta south (β1S), and beta southeast (β1SE). The number 1 following β, is to indicated that the zone is in the CP1 area, since the beta reservoir is encountered throughout the field.

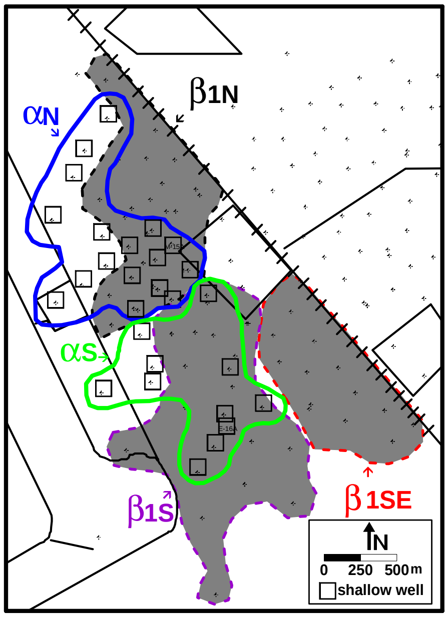

*Figure 1. Zones of CP1 area.*

Northern CP1 wells completed above 1450m depth are considered to be in the αN zone, those open deeper are in β1N. Southwestern wells completed above 1650m are in αS, those below in β1S. All β1SE wells are open at depths greater than 1900m, as shown in Figure 2. To characterize each of the CP1 reservoir zones the behavior of their production wells was considered.

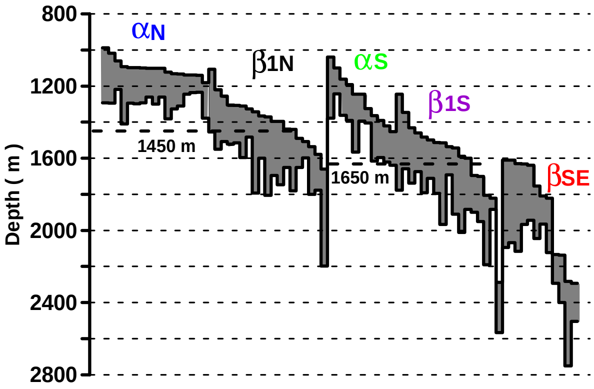

*Figure 2. CP1 Well Completions*

## RESERVOIR CHARACTERISTICS

The Cerro Prieto geothermal field is limited by the Cerro Prieto (FCP) and Imperial faults, which are about 15 km apart. The shape and size of the reservoir is reflected by the distribution of hydrothermal mineral zones (Elders et al., 1981). The top of the β reservoir is defined by that of the silica and epidote zone (Figure 3). The normal Fault H (FH) which is clearly defined in the figure, is considered to be the main geothermal fluid conduit in the system (Halfman et al., 1982, 1986; Lippmann et al., 1991).

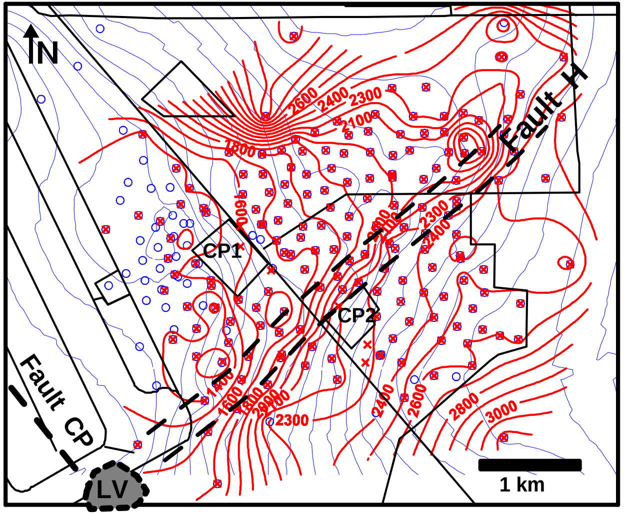

LV = Laguna Volcano

*Figure 3. Top of silica and epidote zone (depth in m).*

Toward the southwest, in the Laguna Volcano (LV) area (Figure 3) where FH intersects FCP, the main surface manifestations of the field are found.

## MASS FLOW, STEAM QUALITY AND ENTHALPY

It is possible to calculate how many times the fluid contained in the reservoir pores has been removed and replaced since 1973 if for each CP1 reservoir zone, an area, a thickness, a porosity of 0.12 and a fluid density of 750 kg/m$^3$ (corresponding to saturated pure liquid water at 280°C) are assumed (Table 1). The values given in the table confirm the large natural fluid recharge to the reservoir that contributes to the sustainability of the resource (Truesdell et al., 1998).

*Table 1. Volumetric calculations for CP1 reservoir zones.*

| Zone | Area ( km$^2$) | Thickness ( m ) | Mass removed since 1973 (ton x 10$^6$) | Pore volumes removed |
|---|---|---|---|---|
| αN | 1.04 | 300 | 231 | **8.2** |
| β1N | 1.04 | 300 | 162 | **5.8** |
| αS | 0.84 | 300 | 102 | **4.5** |
| β1S | 1.40 | 300 | 165 | **4.4** |
| β1SE | 0.80 | 400 | 143 | **5.0** |

The steam production history for each reservoir zone is given in Figure 4. It illustrates how and where production increased in CP1 with time.

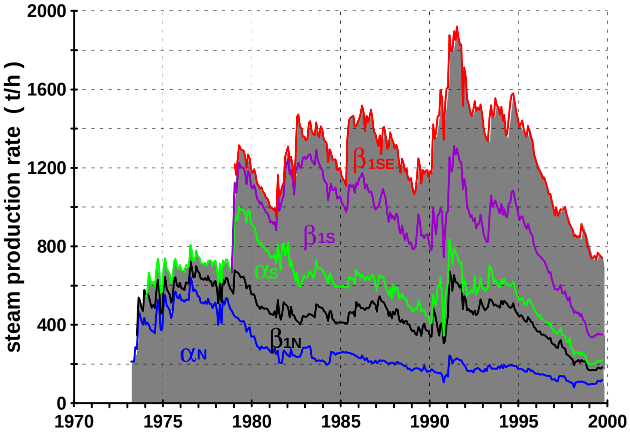

*Figure 4. Steam production history for CP1 reservoir zones.*

To emphasize trends, for each CP1 reservoir zone the average steam production per well (ASPPW) is given in Figure 5. To emphasize trends, the calculated linear fit to the last five-year data is also shown. In 1980, the ASPPW was above 50 t/h for all zones, except for αN where it was lower (about 30 t/h). However, the decline rate in αN is smaller than in other zones. At present (1999), the ASPPW for β1N and β1S is about 10 t/h, which is lower than that of αN (about 15 t/h). The highest 1999 ASPPW is found in the β1SE zone (about 41 t/h), from which about half of the total CP1 steam is produced.

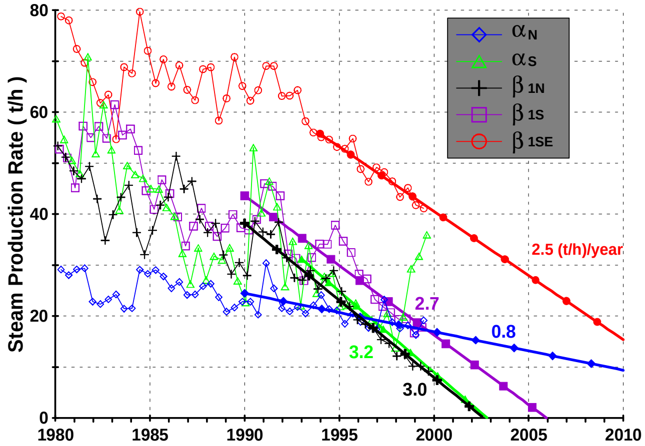

*Figure 5. Average steam production per well for CP1 reservoir zones.*

The production enthalpy for each CP1 reservoir zone and a linear fit to the last five-year data is shown in Figure 6. In each zone the trends in enthalpy and ASPPW are similar. Clearly, the enthalpy of the produced fluids decreased in all CP1 zones during the 1994-99 period, especially in β1N and αS.

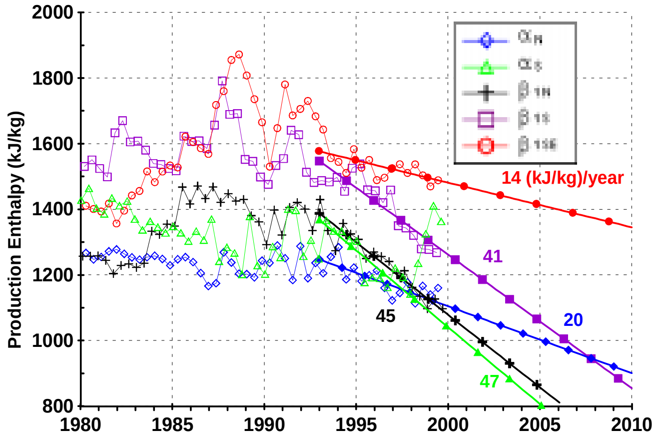

*Figure 6. Production enthalpy history for CP1 reservoir zones.*

## CHEMICAL AND ISOTOPIC CHANGE

As result of the inflow of cold groundwater into CP1 reservoir, Cl and $\delta^{18}$O have decreased since production started in 1973. After the second half of 1989, when reinjection started, the Cl and $\delta^{18}$O values changed in some of the CP1 reservoir zones.

In order to illustrate the changes in fluid chemistry due to the influx of cold, more diluted groundwaters just before the effects of the highly concentrated injectate, only 1989 data are shown.

Distribution of Cl at reservoir conditions (Truesdell et al., 1989) and $\delta^{18}$O at total discharge for the CP1 area in 1989, are shown in Figures 7 and 8, respectively. Geochemical and isotopic data for Cerro Prieto have been presented previously (e.g., Stallard et al., 1987; Truesdell et al., 1989; Verma et al., 1996; Truesdell and Lippmann, 1998).

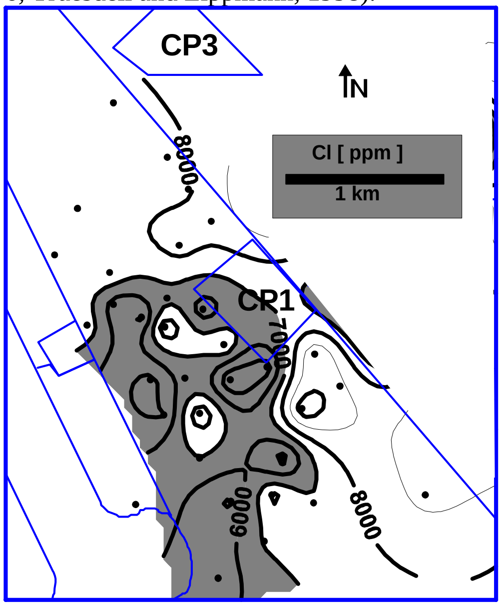

*Figure 7. Reservoir chloride concentrations (in ppm) for 1989.*

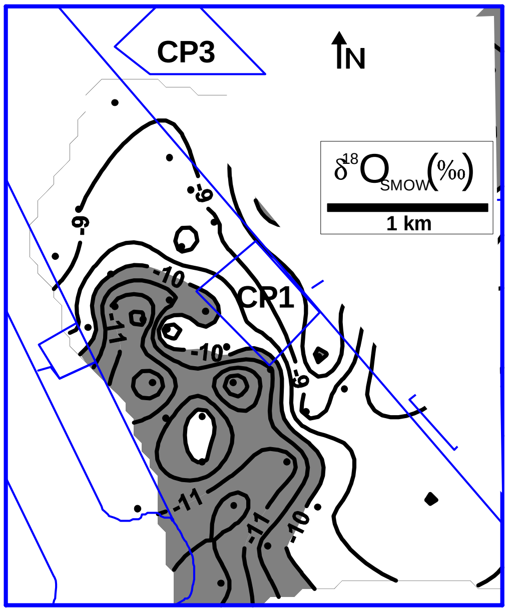

*Figure 8. Total discharge $\delta^{18}O_{SMOW}$ (‰) for 1989.*

According the geochemical evolution, lower Cl and $\delta^{18}O$ values (i.e., Cl < 6000 ppm and $\delta^{18}O < -11$) had been presented in the southwest margin of the CP1 area (e.g. in 1989 Figs. 7 and 8 ). On the other hand, the highest reservoir temperatures, as indicated by the NaKCa geothermometer, have been observed toward the southern part of CP1 (Figure 9), where more dilution occur.

This suggests that in the south the α and β reservoirs are in hydraulic communication with shallow, light-groundwater aquifers and deep hot water recharge zones. A good communication between shallow (αS) and deeper (β1S) reservoir zones is also inferred.

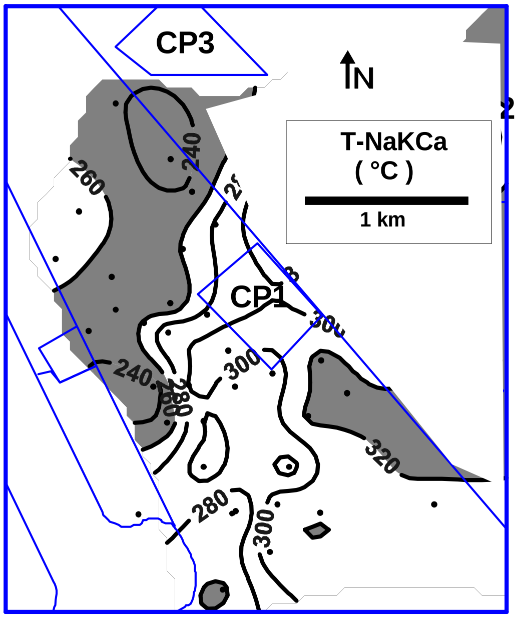

*Figure 9. NaKCa geothermometer temperatures (in °C) for 1989.*

The CP1 wells produce almost entirely liquid-phase fluid. Higher enthalpies are obtained from wells in the southern CP1 area, which is an indication of higher temperatures. Enthalpy distribution agrees with that of the NaKCa geothermometer temperatures.

Although it has been more exploited, the northern CP1 zone shows less dilution than the southern zone, as indicated by the Cl and $^{18}O$ data. This is due to the influence of a large aquifer on the northern CP1 area, whose water has a Cl concentration similar to that of the production zones, but lower NaKCa geothermometer temperatures.

In accord with previous fluid flow models of the Cerro Prieto geothermal system (e.g., Lippmann et al., 1991), the geothermal fluids discharged to the west, in an area of surface manifestations southwest of the field. However, west and northwest of CP1 zone, there were no significant surface manifestations. This situation allows that hot fluids form a large shallow aquifer.

In the northwest, the large shallow aquifer formed, was partially insolate with more diluted water, could be due to the lack of surface fluid discharge. So, it is suggested that the shallow aquifer formed was cooled by conduction (i.e., no by mixture), so their waters were re-equilibrated to form its low NaKCa geothermometer, but the Cl and $\delta^{18}O$ values was conserved. As results to reservoir exploitation in north of CP1, the sallow aquifer has been recharging the north CP1 reservoirs showing lower dilution and NaKCa geothermometer than south reservoirs in CP1.

## INJECTATE RETURNS

In 1989, cooled pond brines began to be injected into the reservoir. As a result of the evaporation process in the separators and the Cerro Prieto evaporation pond, the reinjected fluid is enriched in chlorides and the water of heavy isotopes. These conservative species can be used to trace the movement of the injectate. The chlorides in the water for short-term (e.g., weekly), and the isotopes, specially deuterium, for long-term (e.g., yearly) monitoring.

In Cerro Prieto, deuterium isotope is used as injectate tracer more than $\delta^{18}O$.

The lack of a deuterium shift from exchange with rock minerals, make deuterium more useful than $\delta^{18}O$ to trace reinjection front, but also to determine the inflow of cold water recharge. Due to the origin of fluid reservoir composition, the surrounding groundwater have lower deuterium composition than reservoir fluids (Truesdell et al., 1981). Here only some interesting facts related to reinjection are considered, using Cl and deuterium values.

The 303 reinjection well is completed in the αN zone, as are the 301 and 302 production wells (Figure 10). According to the chloride data (Figure 11), there is good horizontal hydraulic communication between the injector 303 and the producers 301 and 302, but not with the nearby M-114 production well, which is completed in the β1N zone. For more details, including the effect of 303 injection on the steam flow rate of these producers, see Truesdell et al. (1999).

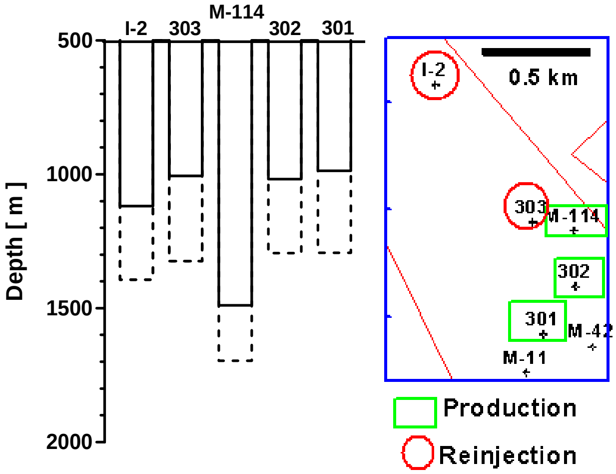

*Figure 10. Location and completion of injection and production wells in the northern part of CP1.*

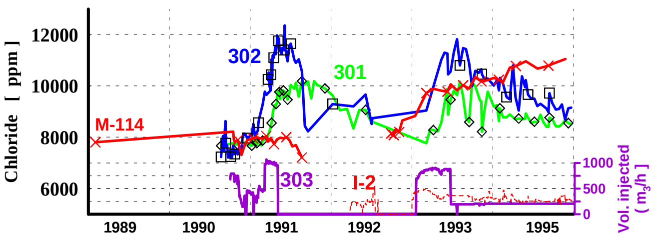

*Figure 11. Chloride concentration histories of production wells close to the 303 injector.*

To the south, injection wells 101 and M-48 are completed in the αS zone, as is the M-50 producer. However, most of the neighboring production wells are completed in zone β1S (Figure 12).

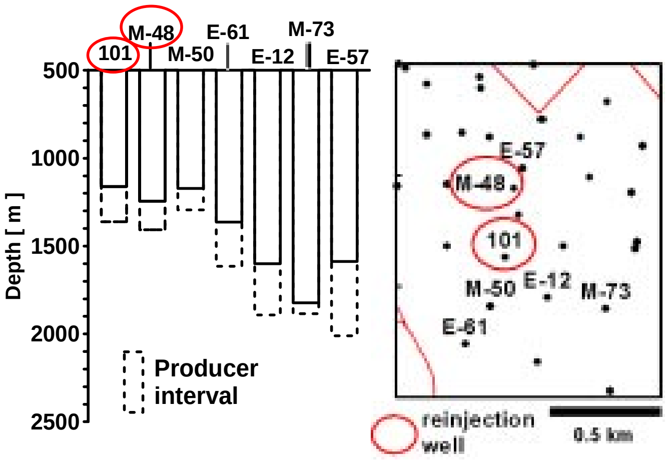

*Figure 12. Location and completion of injection and production wells in the southern part of CP1.*

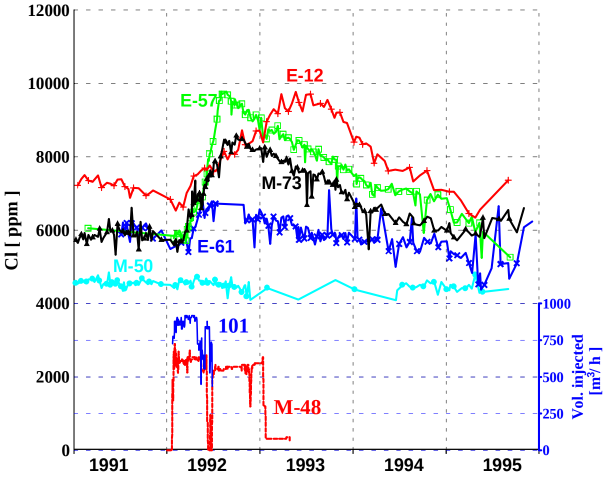

*Figure 13. Chloride concentration histories of production wells close to injectors 101 and M48 wells.*

Fluids produced by wells open in the βSl zone, had an increase of Cl concentration (Figure 13), indicating injectate returns from wells 101 and M-48. According to the completion of M-73 and 101, the injected fluid flowed down more than 500 m over a half-a-kilometer horizontal distance.

Production well M-50 did not show an increase in chlorides although E-61 located beyond M-50 (Figure 12), showed one (Figure 13).

A general overview of injectate returns can be obtained from the distribution of deuterium (Figure 14). In the northwestern part of CP1, isotopic heavy fluid (i.e., δD>-90 ‰) injected into the "I-series" wells moves towards CP1 north and the northwest of the CP3 area. Reinjected fluids from well E-6, move from the south of CP1 to central area of CP2. Isotopic light water (i.e., δD<-100 ‰) indicate inflow of colder groundwaters.

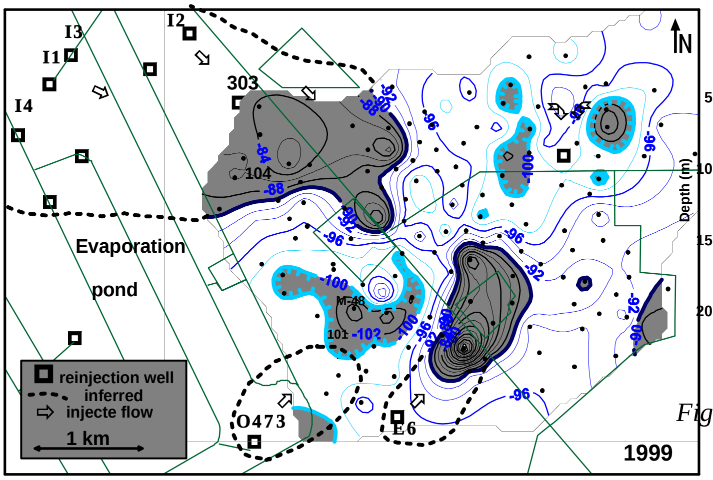

*Figure 14. Distribution of δD (‰) calculated at total discharge in 1999.*

## WATER LEVELS, PRESSURE HISTORY AND DOWNHOLE TEMPERATURES

In 1973, when the first power unit came on line, the water level was similar (i.e., within a 50 m range) in all CP1 reservoir zones. Since then, the northern zones αN and β1N have shown the smallest water level declines in spite of being the ones most exploited in CP1. The largest water level declines (i.e., pressure drawdowns) have been observed in the southern CP1 reservoir zones.

Three wells located in the northern CP1 were selected to show the changes in temperature in both geothermal reservoirs. The static downhole temperature logs given below (Figures 15 and 16) are considered to be representative of the temperature in that part of the field.

Between 1984 and 1994, well E-9 showed temperature decreases of about 20°C in the αN zone (above 1450m depth), and of about 50°C in the β1N zone below. Similar temperature changes were observed in well E-63 between 1989 and 1997.

Well 143, drilled in 1998, shows a temperature reversal below 1800m depth. The reversal is perhaps due to the intense cold water recharge into the reservoir in response to the high rate of production in the CP3 area, as discussed in the next section (i.e., CP1 fluid flow model).

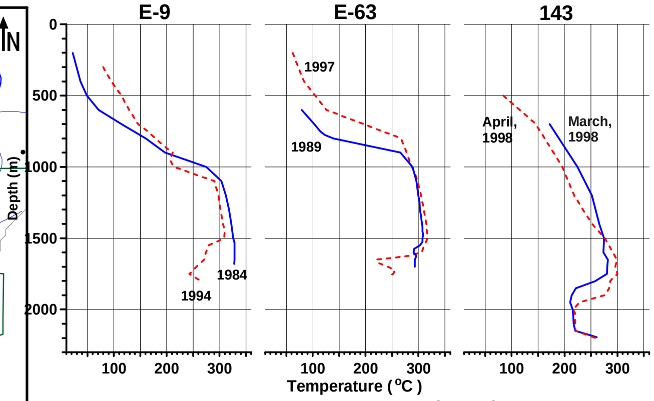

*Figure 15. Downhole temperature profiles for wells E-9, E-63 and 143.*

For the αS and β1S reservoir zones, two pairs of wells located close together were selected to show changes in reservoir temperatures. This allows to follow temperature changes in time, which indicate significant reservoir cooling.

The temperature logs in wells M-48 and E-57, obtained between 1978 and 1989, are shown in Figure 16. The temperature change in the αS reservoir zone is more than 80°C, but in the β1S zone it is less than 80°C. Similar cooling has been observed in both of these zones in wells M-84 and M-84A during the 1978-1998 period (Figure 16).

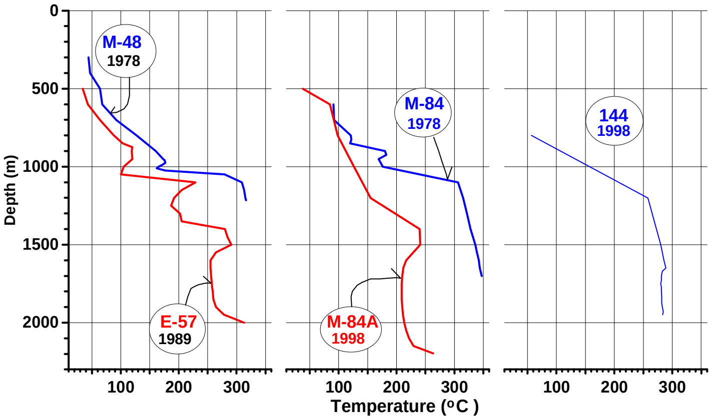

*Figure 16. Temperature profiles for wells M-48, E-57, M-84, M-84A and 144.*

However, there is a reservoir zone in CP1 which has been less affected by cooling. Well 144 is completed in the β1SE reservoir zone. In 1989 its temperature below 1500m depth was about 280°C and did not present a temperature reversal. The temperature in the β1SE reservoir zone is the highest in CP1.

## CP1 FLUID FLOW MODEL

On the basis of the reservoir engineering and production data reviewed above, a fluid flow model for the CP1 area was developed. The model is shown using three cross-sections; their location are given in Figure 17. In order to emphasize the change in fluid flow direction, snapshops of the model are presented for two different times, one for 1973 (when commercial production began) and one for 1999.

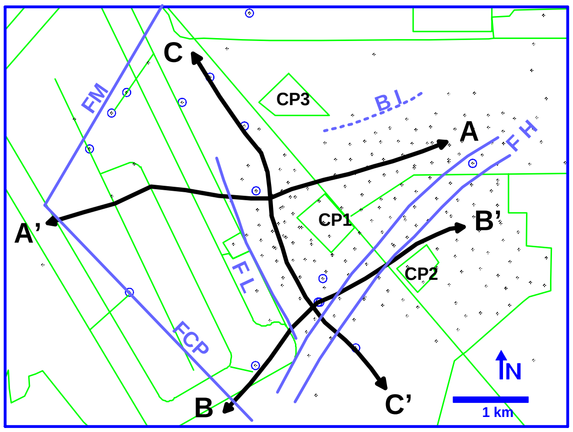

*Figure 17. Location of cross-sections. FM= Michoacán Fault; FCP = Cerro Prieto Fault (from Corona Ruíz, 1996); FH= Fault H; FL= Fault L (from Lippmann et al., 1991); BI= Impermeable barrier at production depth.*

Between FCP and Fault L there is a shallow aquifer which we called sigma (σ); see cross section A-A' in Figure 18. This aquifer corresponds to a sandstone formation located between wells M-9 and M-6 at 500-700m depth (Halfman et al., 1982, Figs. 6A and 8A). Toward the southern part of CP1 the σ aquifer is limited because the two faults are closer together than in north. On other hand, the model indicates that only close to the CP3 area there is some vertical permeability between the αN and β1N reservoir zones.

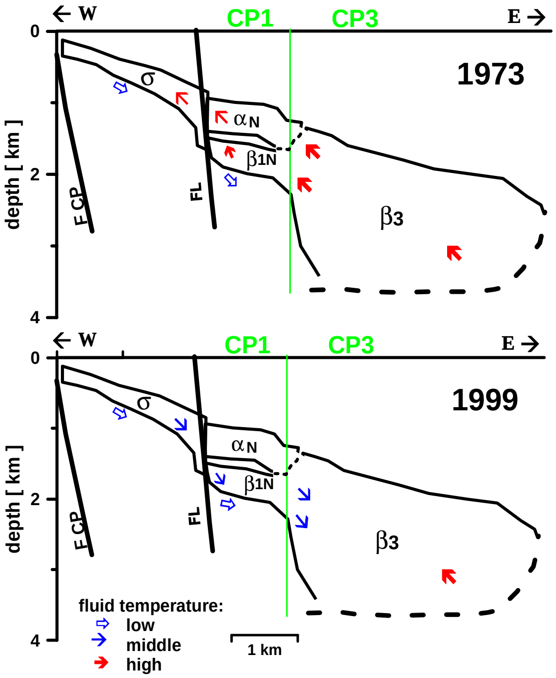

*Figure 18. CP1 fluid flow model. Cross-section A-A', for 1973 and 1999.*

There exists more hydraulic communication between the β1N and β3 zones than between zones αN and β3. Due to the high rate of production in CP3 area (i.e., from the β3 reservoir zone) and because of the presence of an impermeable barrier (BI) to the north, most fluid recharge to β3 zone, is through the β1N zone. This causes more inflow of cold water into β1N than into the αN zone, which comes from the σ aquifer. Although the αN zone has been subjected to more exploitation than β1N, it has shown less cooling than the β1N zone. This situation has been reflected in the changes in steam production, enthalpy, fluid geochemistry, pressure and downhole temperatures.

Because the recharge water from the σ aquifer is cooler and denser it tends to flows down into β1N zone, in the northern CP1 area. This also occurs because the head pressure in the β1N reservoir zone is lower than in αN.

During the 1973-1999 period, the pressure drop in CP1 was between 30 to 70 bars; in CP2 and CP3, it was between 50 to 80 bars. This situation produces a reversal in flow direction, however the fluids follow the same paths.

Some characteristics of the model along the B-B' section (Figure 19) are the high vertical permeability between zones αS and β1S, and the limited recharge from the aquifer σ, when compared to the northern CP1 area (i.e., section A-A').

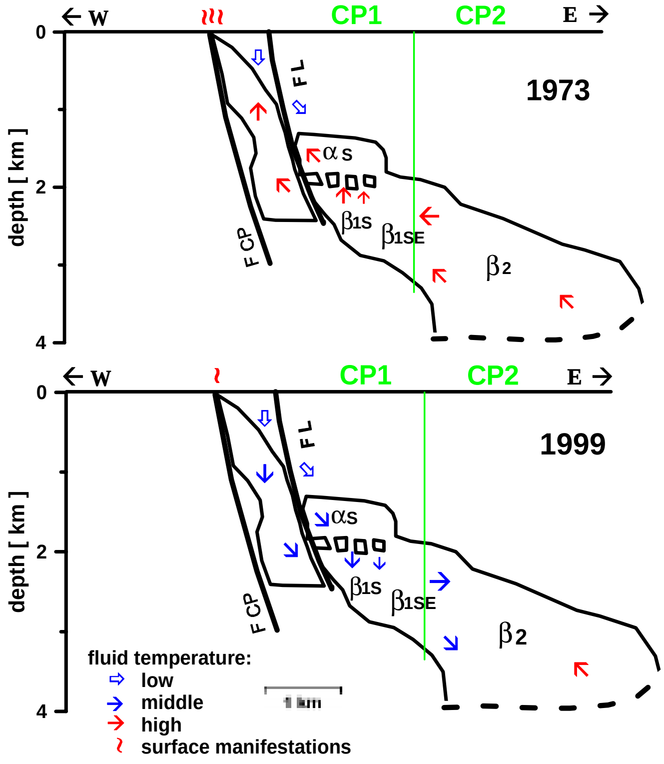

*Figure 19. CP1 fluid flow model. Cross-section B-B', for 1973 and 1999.*

Cross-section B-B' shows that reservoir zones β1S and β1SE receive more recharge than the αS zone. Production in the CP2 area induces fluid recharge from the β1S and β1SE zones. Because it is in hydraulic communication with these two zones, the αS reservoir zone is affected by the exploitation of the CP2 area (i.e., of the β2 reservoir zone). Zones αS, β1S and β1SE have cooled as groundwater flows through them towards the CP2 area (i.e., cooling has been observed in these three CP1 reservoir zones).

On other hand, in the northern CP1 area, the inflow of groundwater induced by CP3 production is channeled mainly through β1N, thus presenting significant cooling.

Cross-section C-C' (Figure 20) shows that in 1999 the direction of fluid flow along the permeable conduits is opposite to that in 1973. The model indicates than in the northern CP1 fluids tend to move more horizontally than vertically, while in the south the vertical fluid movement predominates.

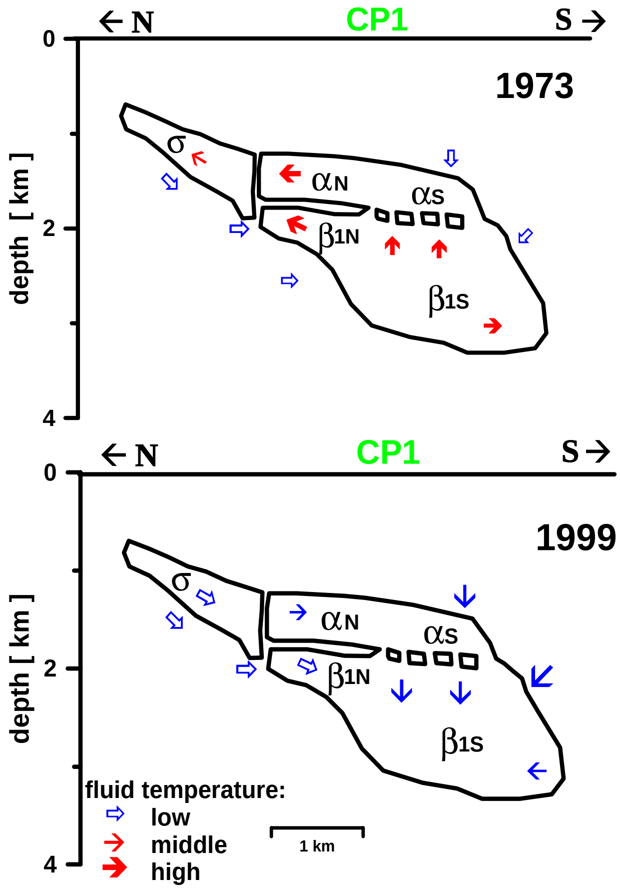

*Figure 20. CP1 fluid flow model. Cross-section C-C', for 1973 and 1999.*

Section C-C' shows that in the north the groundwater recharge from the σ aquifer occurs at shallow depth. In the southern CP1 area, the main hotter recharge is at depth (i.e., through zone β1S).

## CONCLUSIONS

The geothermal reservoirs in the CP1 area can be subdivided into five zones that respond to exploitation according to the hydraulic communication among the zones and with the shallow σ groundwater aquifer.

The updated fluid flow model for the CP1 area integrates the main geological and hydrological characteristics of the Cerro Prieto field.

In the northern part of CP1, the effects of the inflow of cold water is intensified in the β1N reservoir zone, causing its large decline in steam production. On the other hand, the αN reservoir zone has the most stable production condition of all CP1 reservoir zones. This is explained by its small communication with the CP3 production area and by the recharge support it receives from the σ aquifer.

Chemical evidence indicate that in the southern CP1 area. the α and β reservoirs had good hot water recharge from depth as well as good groundwater recharge before exploitation began. The αS, β1S and β1SE reservoir zones showed more diluted waters (i.e., lower chloride concentrations and isotopically light waters) than in the north, but also higher NaKCa geothermometer temperatures and enthalpy than the northern zones.

The updated model explains the reversal of temperatures with depth developed in the northern CP1 area. It also shows that the αS reservoir zone receives limited recharge which results in large pressure drawdowns, causing it to be almost taken out of production.

Because zone β1SE does not have direct cold water recharge, it is the one showing the highest temperature and best steam production conditions in the CP1 area. At present, about 50% of the total steam produced by CP1 wells comes for this particular zone.

## ACKNOWLEDGEMENTS

We thank Marcelo Lippmann and Alfred Truesdell for their review of the manuscript and useful comments.

## REFERENCES

Corona Ruíz, M., (1996). Actualización del modelo geológico del campo geotérmico de Cerro Prieto. Comisión Federal de Electricidad Internal Technical Report RE-009.

Elders, W.A., Hoagland, J.R. and Williams, A.E. (1981). Distribution of hydrothermal mineral zones in the Cerro Prieto geothermal field of Baja California, Mexico. Geothermics, 10, 245-253.

Grant, M.A., Truesdell, A.H., and Mañón, A., (1984). Production induced boiling and cold water entry in the Cerro Prieto geothermal reservoir indicated by chemical an physical measurements. Geothermics, 13, 117-140.

Halfman, S.E., Lippmann, M.J., Zelwer, R., and Howard, J.H. (1982). Fuid flow model of the Cerro Prieto geothermal field based on well log interpretation. Proc. 4th Symp. Cerro Prieto Geothermal Field, Guadalajara, México, August 10-12, 1982. Comisión Federal de Electricidad, pp. 783-798.

Halfman, S.E., Mañón, A. and Lippmann, M.J. (1986). Update of the hydrogeologic model of the Cerro Prieto field based on recent well log data. Geothermal Resource Council Trans., 10, 369-375.

Lippmann, M.J., Truesdell, A.H., Halfman-Dooley, S.E. and Mañón M., A. (1991). A review of the hydrogeologic-geochemical model for Cerro Prieto. Geothermics, 20, 39-52.

Mercado, S. (1976). Movement of geothermal fluids and temperature distribution in the Cerro Prieto geothermal field, Baja California, Mexico. Proc. 2nd United Nations Symposium on the Development and Use of Geothermal Resources, San Francisco, CA, May 20-29, 1975, pp. 487-494.

Sánchez R., J. and de la Peña L., A. (1981). Geology of the Cerro Prieto geothermal field. Proc. 3rd Symposium on the Cerro Prieto geothermal field. Berkeley, Lawrence Berkeley Laboratory Report LBL-11967. pp 309-323.

Stallard, M. L., Winnet, T.L., Truesdell, A.H., Coplen, T.B., Kendall, C., White, L.D., Janik, C.J. and Thompson, J.M. (1987). Patterns of change in water isotopes from the Cerro Prieto geothermal field 1977-1986. Geothermal Resources Council Trans., 11, 203-210.

Truesdell, A.H., Mañón, A., Jiménez , M.E., Sánchez, A., and Fausto, J.J. (1979). Geochemical evidence of drawdown in the Cerro Prieto geothermal field. Geothermics, 8, 257-265.

Truesdell, A.H., Thompson, J.M., Coplen, T.B., Nehring, N.L. and Janik, C.J. (1981). The origin of the Cerro Prieto geothermal brine. Geothermics, 10, 225-238.

Truesdell, A. , Terrazas, B., Hernández, L., Janik, C., Quijano, L. and Tovar, R. (1989). The response of the Cerro Prieto reservoir to exploitation as indicated by fluid geochemistry. Proc. CFE-DOE Symp. In Geothermal Energy, DOE CONF 8904129, pp. 123-132.

Truesdell, A.H., Lippmann, M.J. and Gutiérrez Puente, H. (1997). Evolution of the Cerro Prieto reservoirs under exploitation. Geothermal Resources Council Trans., 21, 263-270.

Truesdell, A.H. and Lippmann, M.J. (1998a). Effects of pressure drawdown and recovery on the Cerro Prieto Beta reservoir in the CP-III area. Proc. 23rd Workshop on Geothermal Reservoir Engineering, Stanford, CA, pp. 90-98.

Truesdell, A.H., Lippmann, M.J, Gutiérrez P., H. and de León V., J. (1998b). The importance of natural fluid recharge to the sustainability of the Cerro Prieto resource. Geothermal Resource Council Trans., 22, 529-536.

Truesdell, A.H., Lippmann, M.J, de León, J. and Rodríguez, M.H. (1999). Cerro Prieto cold water injection: Effects on nearby production wells. Geothermal Resource Council Trans., 23, 367-374.

Verma, M., Quijano, L., Gutiérrez, H., Iglesias, E. and Truesdell, A.H. (1996). Isotopic changes in the fluids of the Cerro Prieto Beta reservoir. Proc. 21th Workshop on Geothermal Reservoir Engineering, Stanford, CA, pp. 93-99.